

# Constraining dark energy models using Jackknife and Bootstrap resampling

Roshna K,\* Nikhil Fernandes, P Praveen, and V. Sreenath†

*Department of Physics, National Institute of Technology Karnataka, Surathkal, Mangaluru 575025, India.*

Analyses of type Ia supernovae have helped us shed light on the existence and nature of dark energy. Most of these analyses have relied on Bayesian techniques. In this work, we rely on resampling techniques to analyse supernova data. In particular, we use the generalised least squares method together with jackknife and Bootstrap techniques to estimate parameters of  $\Lambda$ CDM, flat  $\Lambda$ CDM,  $w$ CDM, flat  $w$ CDM, and flat  $w_0 w_a$ CDM models from the recent PantheonPlus and SH0ES data. For completeness, we also perform Bayesian analysis using Markov chain Monte Carlo (MCMC) and nested sampling algorithms, and compare the results. We note that resampling techniques can help highlight the limitations of the data. For instance, we see that the Jackknife method estimates a strong positive correlation between  $h$  and  $M$  and higher standard deviations for both. This may have significant implications for the Hubble tension. We conclude with a discussion of our results.

## I. INTRODUCTION

Observations of distant Type Ia supernovae (SNe Ia) have provided the first evidence for the late-time accelerated expansion of our Universe [1, 2]. This accelerated expansion is attributed to dark energy, which currently dominates the universe’s energy density. The exact nature of dark energy remains a mystery. The simplest explanation for dark energy is that it is a cosmological constant  $\Lambda$ , described as a constant energy density with negative pressure, corresponding to an equation-of-state parameter  $w = -1$  [3]. Together with the idea of cold dark matter, it leads to the standard model of cosmology, known as the  $\Lambda$ CDM model.

Despite the success of the  $\Lambda$ CDM model in explaining a wide range of observations, recent measurements of Baryon Acoustic Oscillations (BAO) data provided by the Dark Energy Spectroscopic Instrument (DESI) Collaboration, in combination with the Cosmic Microwave Background (CMB), have revealed tensions with that of cosmological constant-like dark energy [4]. These discrepancies suggest the presence of a dynamical dark energy, wherein the equation of state parameter varies with the redshift. Various parametrisations of the dynamical dark energy equation of state parameter  $w(z)$  have been proposed in the literature (see, for instance, [5]). One of the simplest parametrisations of the dynamical dark energy equation of state parameter is a constant  $w(z)$ , but not necessarily equal to  $-1$  (see, for instance, [6–8]). This model of dark energy is referred to as the  $w$ CDM model. A more general parametrisation of the equation of state parameter  $w(z)$  is the Chevallier-Polarski-Linder (CPL) parametrisation, in which  $w(z)$  slowly varies linearly with redshift [9, 10]. This simple and well-known two-parameter model of dark energy is called the  $w_0 w_a$ CDM model. In this model, the equation of state parameter  $w$  evolves with redshift as  $w(z) = w_0 + w_a(1 + z)$ , where  $w_0$  denotes the present value of the equation of state parameter and  $w_a$  describes its evolution with the redshift.

In this work, we investigate these models of dark energy and constrain their model parameters using the state-of-the-art PantheonPlus and SH0ES supernovae dataset [11, 12]. While several studies [13–16] have already provided Bayesian constraints for these models, our goal is to further examine the consistency and reliability of these results by applying different statistical methods.

\*Electronic address: [roshnak.217ph005@nitk.edu.in](mailto:roshnak.217ph005@nitk.edu.in)

†Electronic address: [sreenath@nitk.edu.in](mailto:sreenath@nitk.edu.in)

In this work, we utilize non-parametric resampling techniques [17–19] such as the Jackknife and Bootstrap methods. These resampling techniques involve repeatedly drawing samples from the original dataset and estimating the model parameters. The main advantage of these techniques is that they do not rely on any assumptions about the underlying distribution of the data. We also analyse the dark energy models using both frequentist, Generalised Least Squares (GLS) method, and Bayesian approaches. In the Bayesian approach, we perform analysis using two different sampling algorithms: the Markov Chain Monte Carlo (MCMC) [20], and the advanced nested sampling algorithm [21].

The paper is organized as follows. In Section II, we present the theoretical background and describe the various models of dark energy considered in this work. In Section III, we describe the PantheonPlus and SH0ES dataset used in our analysis. This is followed by Section IV, where we discuss the statistical methods, including frequentist analyses such as GLS and resampling techniques, namely Jackknife and Bootstrap, as well as the Bayesian approach, including MCMC and nested sampling, employed in this study. We present the constraints obtained for each cosmological model using the different methods in Section V. In Section VI, we conclude the paper with a summary and discussion of our results.

## II. THEORETICAL BACKGROUND AND MODELS OF DARK ENERGY

We consider the homogeneous and isotropic Friedmann–Lemaître–Robertson–Walker (FLRW) geometry with the metric,

$$ds^2 = c^2 dt^2 - a^2(t) \left( \frac{dr^2}{1 - \kappa r^2} + r^2 (d\theta^2 + \sin^2 \theta d\phi^2) \right), \quad (2.1)$$

where  $a(t)$  is the scale factor that captures the expansion of the Universe,  $\kappa$  is the spatial curvature that takes values of  $-1, 0, 1$  for an open, flat, and closed Universe. The expansion rate of the Universe is described by the Hubble parameter  $H(z)$  with its present value given by the Hubble constant  $H_0$ . Its evolution with redshift is given by,

$$H(z) = H_0 \sqrt{\Omega_r(1+z)^4 + \Omega_m(1+z)^3 + \Omega_k(1+z)^2 + \Omega_{\text{DE}} f(z)}, \quad (2.2)$$

where  $\Omega_r$ ,  $\Omega_m$ ,  $\Omega_{\text{DE}}$ , and  $\Omega_k$  represent the density parameters for radiation, matter, dark energy, and curvature, respectively, evaluated at the present time. The function  $f(z)$ , which encodes the dynamics of dark energy, is related to the equation of state parameter  $w(z)$  as (see, for instance, [22]),

$$f(z) = \exp \left[ 3 \int_0^z \frac{1+w(z')}{1+z'} dz' \right]. \quad (2.3)$$

The density parameters satisfy the condition  $\Omega_r + \Omega_m + \Omega_k + \Omega_{\text{DE}} = 1$ . In the late universe, contributions from the radiation are negligible. Hence, we will approximate  $\Omega_k = 1 - \Omega_m - \Omega_{\text{DE}}$ . For our analysis, we consider both spatially flat and non-flat cosmological models with different parametrisations of dark energy. We describe these models below.

### A. $\Lambda$ CDM model

In the standard  $\Lambda$ CDM model, dark energy is described by a cosmological constant with an equation of state  $w = -1$ . The Hubble parameter for this model is given by,

$$H(z) = H_0 \sqrt{\Omega_m(1+z)^3 + (1 - \Omega_m - \Omega_{\text{DE}})(1+z)^2 + \Omega_{\text{DE}}}, \quad (2.4)$$

where spatial curvature  $\Omega_k$  is written as  $1 - \Omega_m - \Omega_{\text{DE}}$ . The free parameters in this model are  $\Omega_m$ ,  $\Omega_{\text{DE}}$  and  $H_0$ .

### B. Flat $\Lambda$ CDM model

If we assume a spatially flat Universe with  $\Omega_k = 0$ , the Hubble parameter given in Eqn. 2.4 reduces to

$$H(z) = H_0 \sqrt{\Omega_m(1+z)^3 + (1-\Omega_m)}, \quad (2.5)$$

where  $\Omega_{\text{DE}}$  is written as  $1 - \Omega_m$ . The unknown parameters in this model are  $\Omega_m$  and  $H_0$ .

### C. $w$ CDM model

In the  $w$ CDM model, the equation of state parameter  $w(z)$  is constant and does not evolve with redshift. This is different from the  $\Lambda$ CDM model, where  $w$  is fixed to be  $-1$ . In this model, although the equation-of-state parameter is independent of redshift, it can take any value,  $w(z) = w_0$ . The evolution of dark energy is given by the form,

$$f(z) = (1+z)^{3(1+w_0)}, \quad (2.6)$$

and hence the Hubble parameter corresponding to this model is given by,

$$H(z) = H_0 \sqrt{\Omega_m(1+z)^3 + (1-\Omega_m-\Omega_{\text{DE}})(1+z)^2 + \Omega_{\text{DE}}(1+z)^{3(1+w_0)}}. \quad (2.7)$$

In this model, there are four free parameters, namely  $\Omega_m$ ,  $\Omega_{\text{DE}}$ ,  $w_0$  and  $H_0$ .

### D. Flat $w$ CDM model

For a spatially flat universe with  $\Omega_k = 0$ , the Hubble parameter given in Eqn. 2.7 becomes,

$$H(z) = H_0 \sqrt{\Omega_m(1+z)^3 + (1-\Omega_m)(1+z)^{3(1+w_0)}}. \quad (2.8)$$

The free parameters in this model are  $\Omega_m$ ,  $w_0$ , and  $H_0$ .

### E. Flat $w_0 w_a$ CDM model

In this model, the equation of state of dark energy evolves with redshift as,

$$w(z) = w_0 + w_a \frac{z}{1+z}, \quad (2.9)$$

where  $w_0$  denotes the present-day value of the equation of state and  $w_a$  describes its evolution with the redshift. This parametrisation is also known as the CPL parametrisation [9, 10]. The dark energy evolution function corresponding to this  $w(z)$  is

$$f(z) = (1+z)^{3(1+w_0+w_a)} \exp \left[ -\frac{3w_a z}{1+z} \right], \quad (2.10)$$

and the Hubble parameter is given by

$$H(z) = H_0 \sqrt{\Omega_m(1+z)^3 + (1-\Omega_m)(1+z)^{3(1+w_0+w_a)} \exp \left[ -\frac{3w_a z}{1+z} \right]}. \quad (2.11)$$

In this model,  $\Omega_m$ ,  $w_0$ ,  $w_a$  and  $H_0$  are the free parameters.

### III. OBSERVATIONAL DATASET

In this work, we use the PantheonPlus compilation of Type Ia supernovae, an updated successor to the original Pantheon dataset, which is a comprehensive collection of 18 surveys of supernovae<sup>1</sup>. This dataset includes a sample of 1701 supernovae over the redshift range  $0.001 < z < 2.261$ , including those in galaxies with measured SH0ES Cepheid distances [11, 12]. The dataset also provides the associated measurement errors, represented by a full covariance matrix that combines both statistical and systematic uncertainties. This includes all covariance between SNe Ia and covariance between Cepheid hosts due to systematic uncertainties. We refer to this PantheonPlus and SH0ES dataset as PPS.

For each supernova, the theoretical distance modulus  $\mu(z)$ , which quantifies the difference between an object's apparent magnitude (observed flux  $m$ ) and absolute magnitude (intrinsic brightness  $M$ ), is defined as [23–25],

$$\mu_{\text{theory}}(z) = m - M = 5 \log_{10} \left( \frac{D_L(z)}{\text{Mpc}} \right) + 25, \quad (3.1)$$

where  $D_L(z)$  is the luminosity distance to a supernova with redshift  $z$ . To treat both spatially flat and non-flat cosmological models, the luminosity distance is expressed in its most general form [26],

$$D_L(z) = \frac{c(1+z)}{H_0} \times \begin{cases} \frac{1}{\sqrt{|\Omega_k|}} \sinh \left( \sqrt{|\Omega_k|} \int_0^z \frac{dz'}{E(z')} \right), & \text{if } \Omega_k > 0, k = -1 \text{ (open)} \\ \int_0^z \frac{dz'}{E(z')}, & \text{if } \Omega_k = 0, k = 0 \text{ (flat)} \\ \frac{1}{\sqrt{|\Omega_k|}} \sin \left( \sqrt{|\Omega_k|} \int_0^z \frac{dz'}{E(z')} \right) & \text{if } \Omega_k < 0, k = +1 \text{ (closed)}, \end{cases} \quad (3.2)$$

where  $E(z) = \frac{H(z)}{H_0}$  is the normalised Hubble parameter. To account for the full redshift range of PPS dataset, the theoretical distance modulus is evaluated using  $z_{\text{HD}}$ , the redshift corrected for CMB dipole motion and peculiar velocity [27]. For a given set of model parameters  $\theta$ , the theoretical prediction of the apparent magnitude is,

$$m_{\text{theory}}(z, \theta) = 5 \log_{10} \left[ \frac{3000 \times (1+z)}{h} \times \begin{cases} \frac{1}{\sqrt{|\Omega_k|}} \sinh \left( \sqrt{|\Omega_k|} \int_0^z \frac{dz'}{E(z')} \right) \\ \int_0^z \frac{dz'}{E(z')} \\ \frac{1}{\sqrt{|\Omega_k|}} \sin \left( \sqrt{|\Omega_k|} \int_0^z \frac{dz'}{E(z')} \right) \end{cases} \right] + 25 + M, \quad (3.3)$$

where  $h = H_0 / (100 \text{ km s}^{-1} \text{ Mpc}^{-1})$  is the dimensionless Hubble constant. Note that, on the right-hand side of the Eqn. 3.3, the parameters  $\theta$  enters implicitly via the form of  $E(z)$  as well as through  $\Omega_k$  and  $h$ . For SNe Ia present in the SH0ES Cepheid galaxies, instead of the theoretical apparent magnitude given in Eqn. 3.3, we directly use the Cepheid distance modulus  $\mu^{\text{Cepheid}}$  given

<sup>1</sup> <https://github.com/PantheonPlusSH0ES/DataRelease>

as CEPH\_DIST in PPS dataset. Hence, the theoretical prediction of the apparent magnitude is [12],

$$m_{\text{theory}}(z_i, \theta) = \begin{cases} M + \mu_i^{\text{Cepheid}}, & i \in \text{Cepheid hosts}, \\ m_{\text{theory}}(z_i, \theta), & \text{otherwise.} \end{cases} \quad (3.4)$$

The SH0ES Cepheid distances are included with the hope that it will help to break the degeneracy between the absolute magnitude  $M$  and the Hubble constant  $H_0$ , which cannot be resolved with supernovae data alone. In our analysis, along with the model-dependent parameters discussed in the section II, we also treat the absolute magnitude of Type Ia supernovae,  $M$ , as an additional free parameter.

#### IV. STATISTICAL TECHNIQUES

In this section, we discuss the statistical methods used to estimate model parameters along with the nuisance parameter  $M$ . We perform five different analyses, including methods from both the frequentist and Bayesian approaches. Within the frequentist approach, we apply the GLS<sup>2</sup> method and two resampling techniques, namely the Jackknife and Bootstrap methods. To compare and complement these results, we also conduct two Bayesian analyses using the MCMC and nested sampling algorithms.

##### A. Generalised least squares

This is a standard frequentist statistical method used to get the best-fit parameters of any given model. The fit between theory and data is assessed using the  $\chi^2$  function (see, for instance, [28]), which measures the difference between the theoretical predictions and the observational data. The parameters that best fit the data are identified by minimising the  $\chi^2$  values defined as,

$$\chi^2(\theta) = \Delta m^T C^{-1} \Delta m, \quad (4.1)$$

where  $\Delta m = m_{\text{theory}}(z, \theta) - m_{\text{observed}}(z)$  is the residual vector, and  $C$  is the covariance matrix of the data. For a given model of dark energy with a set of parameters, we can compute the theoretical apparent magnitude  $m_{\text{theory}}$  using Eqn. 3.4. For each parameter  $\theta_\alpha$ , the best fit value of the parameter  $\hat{\theta}_\alpha$  [29] are obtained by minimising the Eqn. 4.1, such that

$$\left. \frac{\partial \chi^2}{\partial \theta_\alpha} \right|_{\theta_\alpha = \hat{\theta}_\alpha} = 0. \quad (4.2)$$

To perform this minimisation, we employ the Py-BOBYQA algorithm [30], a derivative-free optimiser for bound-constrained minimisation problems. It is a Python implementation of the Bound Optimization BY Quadratic Approximation (BOBYQA) solver. The optimization is carried out within the parameter bounds listed in the table I. To estimate the uncertainties associated with the best-fit parameters, we find the curvature matrix  $A$ , which is the second derivative of the  $\chi^2$  function with respect to model parameters [29],

$$A_{\alpha\beta} = \frac{1}{2} \left( \frac{\partial^2 \chi^2}{\partial \theta_\alpha \partial \theta_\beta} \right). \quad (4.3)$$

---

<sup>2</sup> Since we are applying GLS to a non-linear function Eqn. 3.4, we may also call it a non-linear generalised least square.

Parameter	Prior
$\Omega_m$	[0.01, 0.9]
$\Omega_{\text{DE}}$	[-2, 2]
$h$	[0.55, 0.91]
$w_0$	[-4, 4]
$w_a$	[-4, 4]
$M$	[-20, -18]

TABLE I: The lower and upper bounds of model parameters. In the frequentist approach, we limit the search for the best-fitting parameter to this range. In the Bayesian approach, we assume a uniform prior over this range.

The elements of the curvature matrix  $A_{\alpha\beta}$  are evaluated numerically using the central difference formula around the best-fitting parameter. The covariance matrix, which represents the pairwise covariances between each parameter, is then obtained as the inverse of the curvature matrix  $C = A^{-1}$ . The square root of the diagonal elements of  $C$  gives the standard deviation associated with each parameter ( $\sigma_{\alpha}^{\text{GLS}}$ ). In this method, best-fit parameter estimates are obtained without assigning any underlying probability distributions. However, associated variances are estimated by assuming an approximately Gaussian distribution around the minimum.

To plot the confidence regions for any subset of two parameters  $(\theta_{\alpha}, \theta_{\beta})$ , we evaluate the quantity

$$\Delta\chi_p^2(\theta_{\alpha}, \theta_{\beta}) = \sum_{\alpha, \beta=1}^2 (\theta_{\alpha} - \hat{\theta}_{\alpha}) A_{\alpha\beta} (\theta_{\beta} - \hat{\theta}_{\beta}), \quad (4.4)$$

where  $\alpha$  and  $\beta$  vary over the two parameters. The quantity  $\Delta\chi_p^2(\theta_{\alpha}, \theta_{\beta})$  is computed on a two-dimensional grid mapping the plotting range of parameters, and confidence contours are drawn at fixed values of  $\Delta\chi_p^2$ . Since  $\Delta\chi_p^2$  follows a chi-square distribution, for two parameters, the 68% and 95% confidence regions correspond to a  $\Delta\chi_p^2 = 2.30$  and 5.99, respectively. The one dimensional probability distribution for each parameter  $\theta_{\alpha}$  is approximated as a Gaussian and is given as

$$P(\theta_{\alpha}) \propto \exp \left[ -\frac{1}{2} A_{\alpha\alpha} (\theta_{\alpha} - \hat{\theta}_{\alpha})^2 \right]. \quad (4.5)$$

## B. Non-parameteric resampling techniques

Non-parameteric resampling techniques are frequentist statistical methods in which we compute the estimates of interest by creating multiple copies of the original data, either by systematically leaving out one data point at a time or by sampling with replacement. These techniques help us to explore how the results change when we slightly alter the original dataset. These resampling techniques have the added advantage of not requiring assumptions about the data's underlying distribution. In this work, we use two resampling algorithms, the Jackknife and the Bootstrap. Using these resampling techniques, we can compute parameter estimates and assess their uncertainty and bias.

### 1. Jackknife resampling technique

The Jackknife method is a simple resampling technique in which we systematically remove a data point from the original dataset without replacement [31, 32]. This method assesses the stability of

an estimator and quantifies its bias and variance. In this method,  $N$  number of Jackknife samples are created, where  $N$  is the total number of supernovae in the PPS dataset ( $N = 1701$ ). Jackknife resamples are created by systematically removing one observation at a time from the original PPS dataset without replacement. Hence, each of these Jackknife samples contains  $N - 1$  data points. For each of the Jackknife samples, we compute our estimate of the vector of best fit parameters  $\tilde{\theta}_s$  using GLS method described in subsection IV A, and then combine all such estimates to obtain the Jackknife estimate. The vector of Jackknife estimate of parameters  $\hat{\theta}_{\text{jack}}$  [33], is given by,

$$\hat{\theta}_{\text{jack}} = \frac{1}{N} \sum_{s=1}^N \tilde{\theta}_s, \quad (4.6)$$

where  $\tilde{\theta}_s$  is the best fit parameter estimate obtained with each Jackknife subsample. A key aspect of the Jackknife method is that it provides an estimate of the bias of the estimate made using full dataset. The Jackknife estimate of the bias [34] is computed as

$$\widehat{\text{bias}}_{\text{jack}} = (N - 1) (\hat{\theta}_{\text{jack}} - \hat{\theta}), \quad (4.7)$$

where  $\hat{\theta}$  is the mean estimate obtained from the original PPS full dataset. The bias is scaled by the factor  $N - 1$  because each Jackknife sample contains  $N - 1$  data points. If we have the estimate of bias, the Jackknife corrected estimate of the parameter of interest is given by,

$$\hat{\theta}_{\text{jack}}^{\text{corrected}} = \hat{\theta} - \widehat{\text{bias}}_{\text{jack}}. \quad (4.8)$$

The Jackknife covariance matrix is given by [35],

$$C_{\text{jack}} = \frac{N - 1}{N} \sum_{s=1}^N (\tilde{\theta}_s - \hat{\theta}_{\text{jack}}) (\tilde{\theta}_s - \hat{\theta}_{\text{jack}})^T. \quad (4.9)$$

The corresponding Jackknife curvature matrix  $A_{\text{jack}}$  is the inverse of the covariance matrix  $C_{\text{jack}}$ . The Jackknife estimate of the standard deviation of each parameter  $\sigma_{\alpha}^{\text{jack}}$  is given by the square root of the corresponding diagonal element of covariance matrix. To plot the confidence contours for the subset of two parameters  $(\theta_{\alpha}, \theta_{\beta})$  in the Jackknife method, we follow a method similar to that adopted in GLS analysis. In this method, we use the covariance matrix given in Eqn. 4.9 and confidence levels are determined using the  $F$  distribution rather than the  $\chi^2$  distribution. For a set of two parameters, the contour levels corresponding to 68% and 95% confidence regions are obtained from the  $F$  distribution with the numerator degree of freedom  $\nu_1 = 2$  and the denominator degree of freedom  $\nu_2 = N - 2$ , where  $N$  is the number of Jackknife samples. The one dimensional probability distribution of a parameter  $\theta_{\alpha}$  are plotted as a normal distribution with mean  $\hat{\theta}_{\text{jack}, \alpha}^{\text{corrected}}$  and standard deviation  $\sigma_{\alpha}^{\text{jack}}$ .

## 2. Bootstrap resampling technique

The Bootstrap technique [19, 36] involves generating  $B$  number of new Bootstrap samples, each of size  $N$ , which is 1701, by sampling with replacement from the original PPS dataset. This means that in each Bootstrap sample, some data points may repeat, while others may be left out. For each of the  $B$  Bootstrap samples, we compute the best fit parameter estimates using the same  $\chi^2$  minimisation method described in subsection IV A. The Bootstrap mean estimate of the set of parameters  $\hat{\theta}_{\text{boot}}$  [33] is given by,

$$\hat{\theta}_{\text{boot}} = \frac{1}{B} \sum_{s=1}^B \tilde{\theta}_s, \quad (4.10)$$

where  $\tilde{\theta}_s$  is the vector of best fit values obtained for each of the Bootstrap samples. The Bootstrap also provides a way to estimate the bias of the estimator and is given as,

$$\widehat{\text{bias}_{\text{boot}}} = \hat{\theta}_{\text{boot}} - \hat{\theta}. \quad (4.11)$$

The Bootstrap corrected estimate is given by

$$\hat{\theta}_{\text{boot}}^{\text{corrected}} = \hat{\theta} - \widehat{\text{bias}_{\text{boot}}}. \quad (4.12)$$

The Bootstrap estimate of the standard deviation is,

$$\sigma_{\alpha}^{\text{boot}} = \sqrt{\frac{1}{B} \sum_{s=1}^B (\tilde{\theta}_{s,\alpha} - \hat{\theta}_{\alpha})^2}, \quad (4.13)$$

where the subscript  $\alpha$  refers to a parameter of interest and  $\hat{\theta}_{\alpha}$  is the best fit value obtained from the original full PPS dataset. In our analysis, we generated  $B = 1000$  Bootstrap samples. In this method, we directly use the distribution of parameters from the  $B$  Bootstrap samples, after correcting for bias, to plot the confidence contours and do not use the covariance matrix as done in GLS or in the Jackknife method. For any subset of two parameters  $\theta_{\alpha}$  and  $\theta_{\beta}$ , the joint probability contours are estimated using a kernel density estimation (KDE) approach. We use the KDE function available in the `seaborn` module. To plot the one-dimensional distribution of each parameter, we estimate the probability density using a Gaussian kernel density estimator, which is implemented using `gaussian_kde` available in `SciPy`, and we work with the default bandwidth.

### C. Bayesian analysis: MCMC and Nested sampling

In the previous subsections, we discussed the frequentist approach, including the GLS and the two resampling techniques, to constrain parameters of various dark energy models using the PPS dataset. In this section, we carry out our analysis using Bayesian methods. Bayes' theorem provides a systematic way to estimate the model parameters and their associated uncertainties and is stated as (see, for instance, [37]),

$$P(\theta|D) = \frac{P(D|\theta) P(\theta)}{P(D)}, \quad (4.14)$$

where  $P(\theta|D)$  is the posterior probability of the model parameters given the data  $D$ ,  $P(D|\theta)$  is the likelihood which quantifies how probable it is to observe the data given the underlying model parameters,  $P(\theta)$  is the prior information about the parameters, and  $P(D)$  is the normalization constant or evidence. If we assume a Gaussian-distributed dataset, the likelihood is expressed in terms of the  $\chi^2$  as,

$$\mathcal{L}(\theta) \propto \exp(-\chi^2(\theta)/2). \quad (4.15)$$

Thus, in this context, minimizing  $\chi^2(\theta)$  is equivalent to maximizing the likelihood function. To perform the Bayesian analysis, we use two different sampling techniques, namely MCMC and the nested sampling [21]. In the MCMC sampling method, we sample the parameter space and obtain the posterior probability distribution of the model parameters. The sampler generates multiple sequences of points in the parameter space, known as Markov chains. We use the `emcee` Python package [38], which is an ensemble sampler to explore the parameter space. In this work, we assume flat priors for all model parameters as listed in table I. For our analysis, we use 16 chains,

each with 40000 steps. We use the `GetDist` package [39] to analyze the chains after removing the first 30% as initial burn-in. The marginalized mean values and the associated  $1\sigma$  uncertainties are computed with the remaining samples. The convergence of the chains is verified using the **Gelman-Rubin** statistic [40]. We also perform the analysis using the advanced nested sampling algorithm, `PolyChord` [41, 42]. `PolyChord` is designed for exploring higher-dimensional parameter spaces and can efficiently handle multimodal probability distributions. This algorithm works by drawing a set of  $n$  live points uniformly from the prior. At each iteration, the live point with the lowest likelihood is removed and replaced by a new live point with a higher likelihood. We implement `PolyChord` through its Python interface, `pypolychord`<sup>3</sup>, using 250 live points and uniform priors as listed in table I. We set a precision criterion of 0.001 as the convergence threshold. The resulting output samples are analyzed using `GetDist` to obtain the parameter constraints.

Model	Parameter	GLS	Jackknife		Bootstrap	
		$\hat{\theta} \pm \sigma_{\text{GLS}}$	$\widehat{\text{bias}}_{\text{jack}}$	$\hat{\theta}_{\text{corrected}}^{\text{jack}} \pm \sigma_{\text{jack}}$	$\widehat{\text{bias}}_{\text{boot}}$	$\hat{\theta}_{\text{corrected}}^{\text{boot}} \pm \sigma_{\text{boot}}$
$\Lambda$ CDM	$\Omega_m$	$0.297 \pm 0.054$	0.007	$0.289 \pm 0.041$	0.003	$0.293 \pm 0.072$
	$\Omega_{\text{DE}}$	$0.612 \pm 0.080$	-0.067	$0.679 \pm 0.070$	-0.020	$0.632 \pm 0.109$
	$h$	$0.734 \pm 0.010$	-0.010	$0.744 \pm 0.029$	-0.001	$0.735 \pm 0.012$
	$M$	$-19.248 \pm 0.029$	-0.016	$-19.232 \pm 0.087$	0.0009	$-19.249 \pm 0.032$
Flat $\Lambda$ CDM	$\Omega_m$	$0.333 \pm 0.018$	0.036	$0.297 \pm 0.016$	0.013	$0.320 \pm 0.026$
	$h$	$0.735 \pm 0.010$	-0.008	$0.743 \pm 0.029$	-0.0018	$0.737 \pm 0.011$
	$M$	$-19.248 \pm 0.029$	-0.011	$-19.237 \pm 0.087$	0.00004	$-19.248 \pm 0.031$
$w$ CDM	$\Omega_m$	$0.296 \pm 0.074$	-0.182	$0.479 \pm 0.073$	-0.096	$0.392 \pm 0.165$
	$\Omega_{\text{DE}}$	$0.625 \pm 0.762$	0.421	$0.205 \pm 0.605$	0.084	$0.542 \pm 0.524$
	$w_0$	$-0.983 \pm 0.935$	-0.187	$-0.796 \pm 0.779$	-0.520	$-0.463 \pm 1.135$
	$h$	$0.734 \pm 0.010$	-0.009	$0.743 \pm 0.029$	-0.0017	$0.735 \pm 0.012$
	$M$	$-19.248 \pm 0.029$	-0.016	$-19.232 \pm 0.087$	-0.0033	$-19.244 \pm 0.032$
Flat $w$ CDM	$\Omega_m$	$0.288 \pm 0.071$	-0.0002	$0.288 \pm 0.057$	-0.006	$0.294 \pm 0.101$
	$w_0$	$-0.891 \pm 0.148$	0.051	$-0.942 \pm 0.128$	-0.010	$-0.880 \pm 0.213$
	$h$	$0.734 \pm 0.010$	-0.010	$0.743 \pm 0.029$	-0.002	$0.736 \pm 0.012$
	$M$	$-19.248 \pm 0.029$	-0.016	$-19.231 \pm 0.087$	-0.001	$-19.246 \pm 0.032$
Flat $w_0 w_a$ CDM	$\Omega_m$	$0.266 \pm 0.313$	-0.427	$0.693 \pm 0.262$	-0.009	$0.275 \pm 0.145$
	$w_0$	$-0.874 \pm 0.290$	0.483	$-1.357 \pm 0.236$	0.043	$-0.917 \pm 0.199$
	$w_a$	$0.174 \pm 2.120$	0.676	$-0.503 \pm 1.573$	-0.769	$0.942 \pm 1.968$
	$h$	$0.734 \pm 0.010$	-0.010	$0.743 \pm 0.029$	-0.003	$0.736 \pm 0.012$
	$M$	$-19.248 \pm 0.029$	-0.016	$-19.232 \pm 0.087$	-0.002	$-19.246 \pm 0.032$

TABLE II: The table lists the best-fit values and the associated uncertainties of the model parameters obtained with GLS, Jackknife, and Bootstrap. Estimates of best-fit parameters listed under Jackknife and Bootstrap are bias corrected. Jackknife and Bootstrap estimates of bias in the GLS best-fit estimate are also listed. We note that five parameter models are poorly constrained and have higher bias. The parameters  $h$  and  $M$  are equally constrained across models, *i.e.* their standard deviations are same.

<sup>3</sup> <https://github.com/PolyChord/PolyChordLite>

Model	Parameter	MCMC	Nested Sampling
$\Lambda$ CDM	$\Omega_m$	$0.296 \pm 0.054$	$0.297 \pm 0.054$
	$\Omega_{\text{DE}}$	$0.609 \pm 0.080$	$0.611 \pm 0.082$
	$h$	$0.734 \pm 0.010$	$0.734 \pm 0.010$
	$M$	$-19.247 \pm 0.029$	$-19.248 \pm 0.029$
Flat $\Lambda$ CDM	$\Omega_m$	$0.333 \pm 0.018$	$0.333 \pm 0.018$
	$h$	$0.735 \pm 0.010$	$0.735 \pm 0.010$
	$M$	$-19.248 \pm 0.029$	$-19.247 \pm 0.029$
$w$ CDM	$\Omega_m$	$0.241 \pm 0.082$	$0.251 \pm 0.072$
	$\Omega_{\text{DE}}$	$0.697 \pm 0.364$	$0.625 \pm 0.338$
	$w_0$	$-1.156 \pm 0.580$	$-1.299 \pm 0.678$
	$h$	$0.734 \pm 0.010$	$0.734 \pm 0.010$
	$M$	$-19.247 \pm 0.030$	$-19.247 \pm 0.028$
Flat $w$ CDM	$\Omega_m$	$0.286 \pm 0.071$	$0.290 \pm 0.069$
	$w_0$	$-0.908 \pm 0.149$	$-0.913 \pm 0.146$
	$h$	$0.734 \pm 0.010$	$0.734 \pm 0.010$
	$M$	$-19.247 \pm 0.029$	$-19.247 \pm 0.029$
Flat $w_0 w_a$ CDM	$\Omega_m$	$0.322 \pm 0.106$	$0.315 \pm 0.114$
	$w_0$	$-0.919 \pm 0.148$	$-0.913 \pm 0.148$
	$w_a$	$-0.826 \pm 1.35$	$-0.816 \pm 1.398$
	$h$	$0.733 \pm 0.010$	$0.733 \pm 0.010$
	$M$	$-19.247 \pm 0.030$	$-19.248 \pm 0.030$

TABLE III: The marginalised mean and standard deviation of the parameters for the dark energy models obtained using the Bayesian framework, namely, MCMC sampler and nested sampling algorithm. We find that the constraints obtained from both samplers are nearly the same for all model parameters. Here too, we note that parameters  $h$  and  $M$  are equally constrained across models.

## V. OBSERVATIONS

We now present the results of the five different analyses, analyse them, and present our observations. Table II lists the estimates of best-fit values and their standard deviation for various models obtained using GLS, Jackknife, and Bootstrap methods. The best-fit estimates quoted under Jackknife and Bootstrap are bias-corrected. Jackknife and Bootstrap estimates of bias in the GLS best-fit estimate obtained with full PPS data are also provided. From the table, we see that bias for some parameters is large in five-parameter models, namely the  $w$ CDM and flat  $w_0 w_a$ CDM models. From the standard deviation, we see that those parameters are poorly constrained. We also find that, regardless of the model, the bias in estimating  $h$  and  $M$  is low and that their standard deviations are the same across models. Another thing to note is that the biases estimated by the two methods differ.

Marginalised mean values of parameters and their standard deviations obtained using MCMC and nested sampling are provided in Table III. Recall that we have used `emcee` to implement MCMC sampling and `PolyChord` for nested sampling. We provide a comparison of these two Bayesian methods in Figure 1. Figure 1 compares the marginalised contours of parameters of flat  $w_0 w_a$ CDM and  $w$ CDM models obtained using `emcee` and `PolyChord`. We see that, for the models considered here and the priors given in Table I, both methods yield largely similar results. These two models are chosen because they have the most parameters. We have verified that both Bayesian methods agree even better for other models considered in this work.

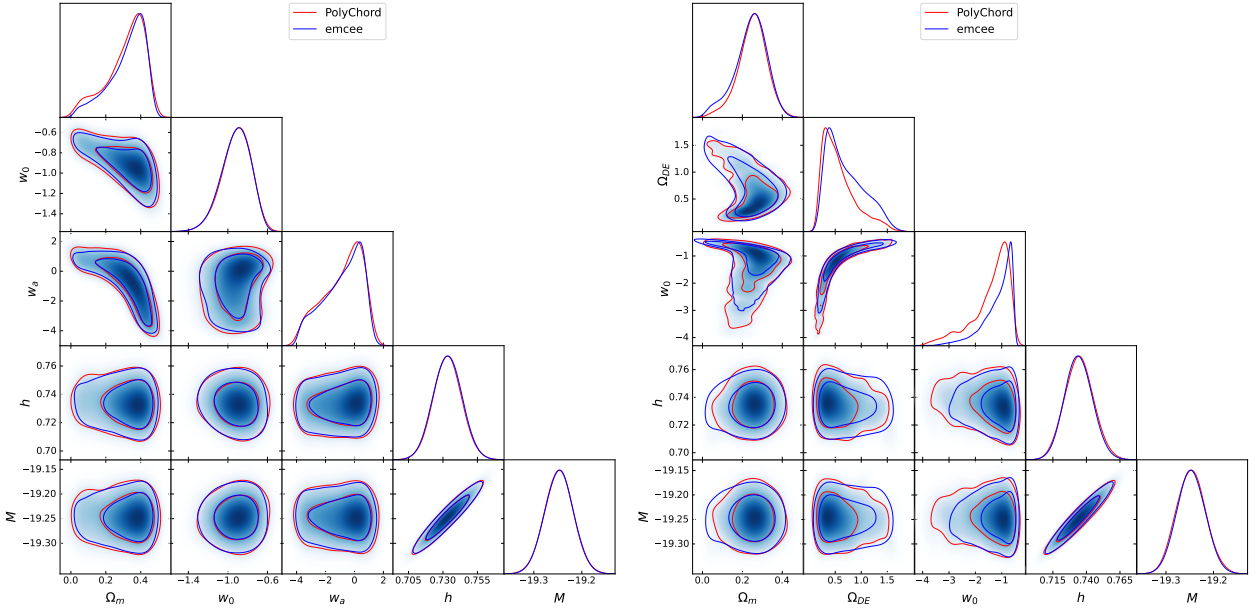


FIG. 1: Figure compares the marginalised confidence contours between different pairs of cosmological parameters in flat  $w_0 w_a$ CDM model (left) and  $w$ CDM model (right) obtained with `emcee` (blue contours) and `pypolycho` (red contours). These two models have been chosen because they have the most parameters. Plots show that both methods largely lead to similar results.

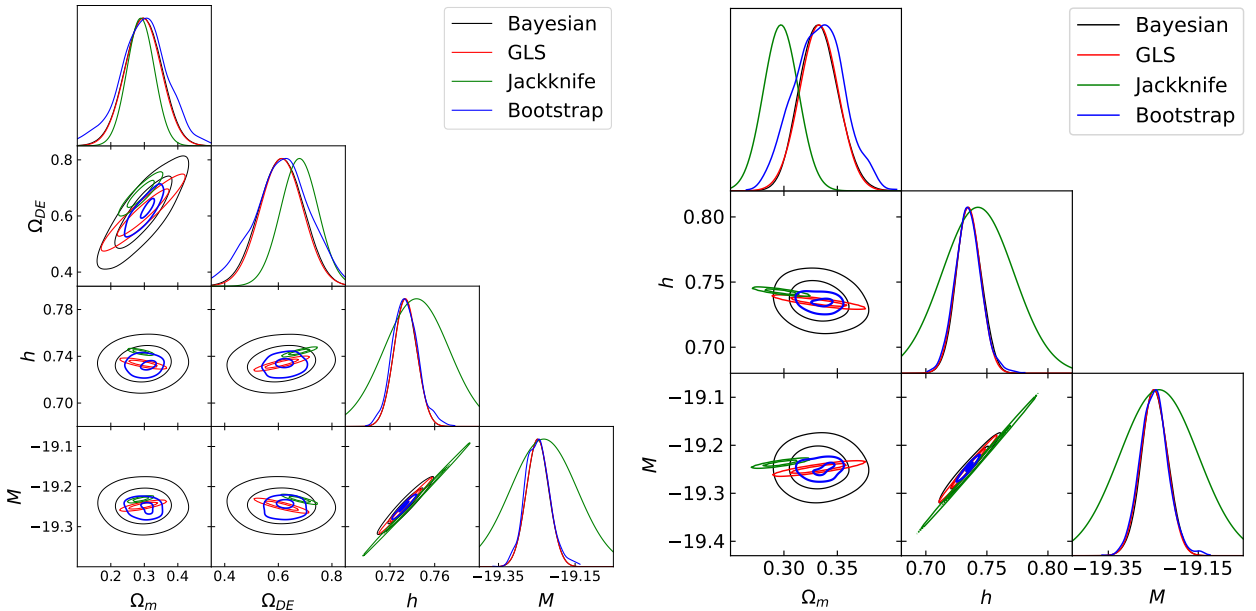


FIG. 2: Corner plots for  $\Lambda$ CDM (left) and flat  $\Lambda$ CDM models (right). Differently coloured contours are obtained by using different methods. Bayesian contours are obtained using `pypolycho`. From two-dimensional confidence contours, we see that the Bayesian contours are more conservative and that all three frequentist methods are consistent with them. An exception is the confidence contour between parameters  $h$  and  $M$ . We find that the Jackknife confidence contour between  $h$  and  $M$  shows a high correlation. With Jackknife, we also find a large standard deviation for these parameters. For the flat  $\Lambda$ CDM model, this alleviates the Hubble tension. In fact, Planck's estimate of  $H_0$  lies well within  $3 - \sigma$  of the estimate using the Jackknife [43]. Further, in the flat  $\Lambda$ CDM model, we note that the bias-corrected Jackknife estimate of  $\Omega_m$  is about  $2\sigma$  lower than the GLS estimate.

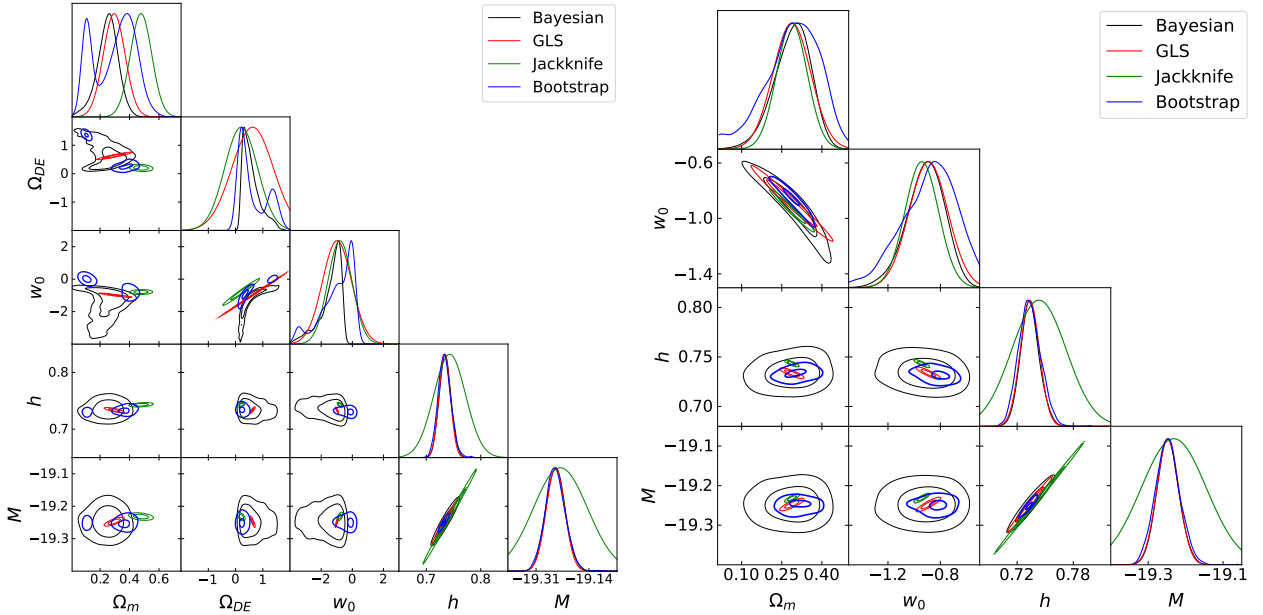


FIG. 3: Same as Figure 2, but for  $w$ CDM (left) and flat  $w$ CDM (right) models. As observed in Figure 2, in general, Bayesian confidence contours are more conservative. An exception is the Jackknife contours for  $h$  and  $M$ , which show high correlation. We also note that the standard deviations of  $h$  and  $M$  are large, allowing a smaller value of  $H_0$ . Above statements hold for both models. For flat  $w$ CDM, results obtained using all methods are consistent. However, for  $w$ CDM model, some of the Jackknife contours, associated with  $\Omega_m$ ,  $\Omega_{DE}$ , and  $w_0$  deviate from other methods. We also note the multimodal behaviour in Bootstrap contours associated with these parameters.

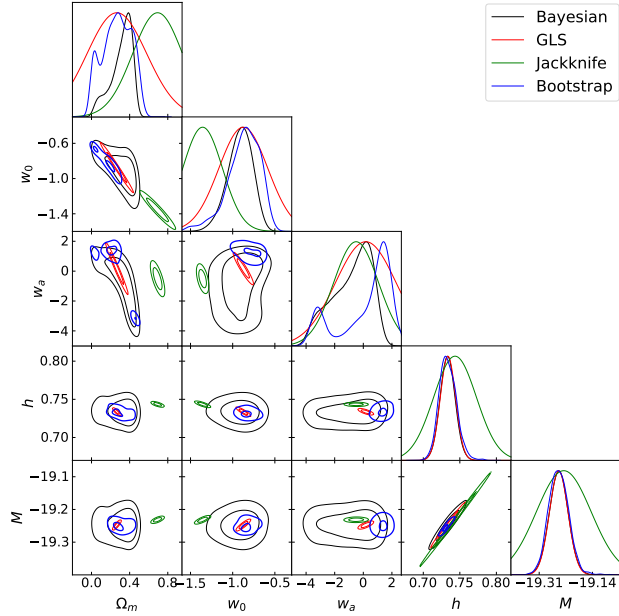


FIG. 4: Same as Figure 2, but for flat  $w_0 w_a$ CDM models. In this figure also, we note that Bayesian contours are, in general, broader. An exception is the case of Jackknife contours in the  $h$  and  $M$  plane, which exhibit high correlation. Further, we note that standard deviation of  $h$  and  $M$  are broader allowing lower values of  $H_0$ . In addition, we note that as in the case of  $w$ CDM model, which also has five parameters, certain jackknife contours involving  $\Omega_m$  and  $w_0$  are not consistent with other methods. We also note that Bootstrap contours and probability distributions for  $\Omega_m$  and  $w_a$  exhibit multimodality.

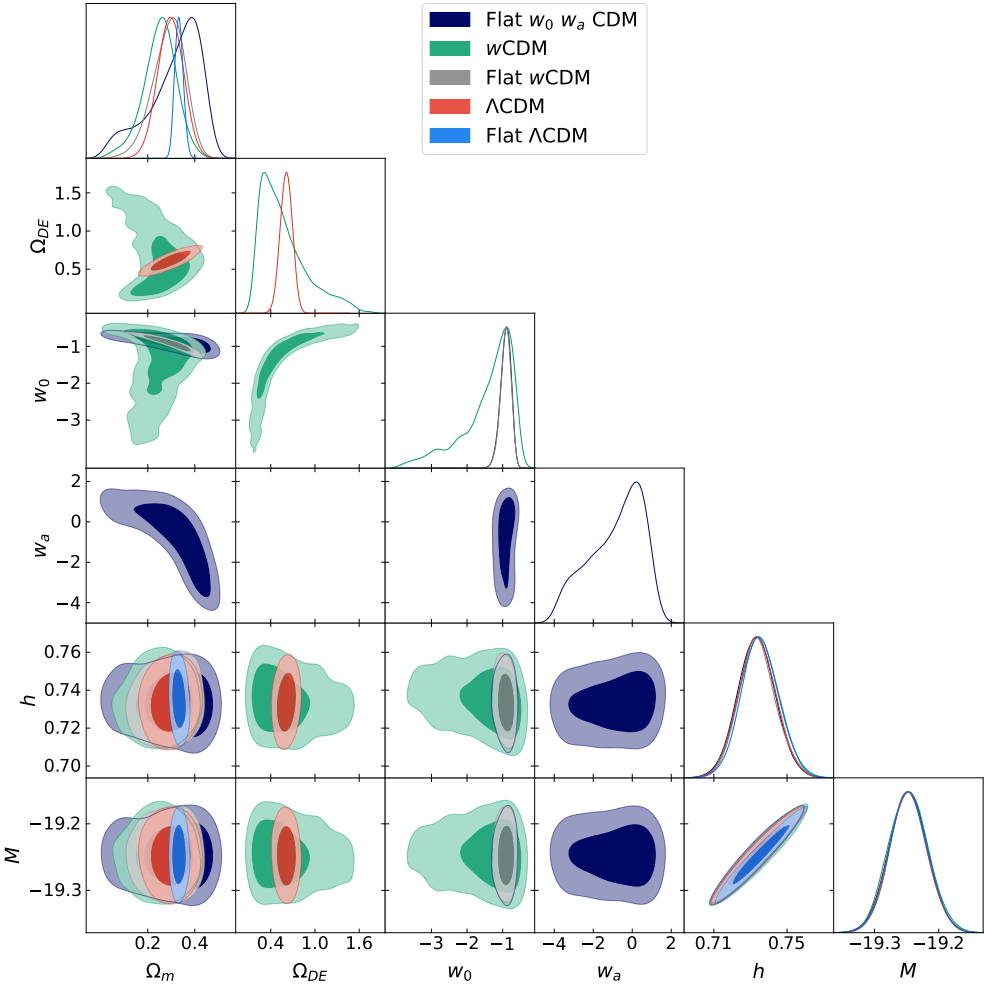


FIG. 5: Figure compares the marginalised confidence contours between different pairs of cosmological parameters for the dark energy models considered in this work, obtained with `pypolychord` nested sampling algorithm. Note that different models have different sets of parameters. Further, since we have not investigated  $w_0 w_a$ CDM model, which has six parameters, there are no contours in  $w_a$  -  $\Omega_{\text{DE}}$  plane. We note with interest that  $\Omega_m$  is best constrained for flat  $\Lambda$ CDM model and that constraints on  $h$  and  $M$  are largely independent of the choice of model.

Figures 2, 3, and 4 compare probability contours of model parameters obtained using GLS, Jackknife, Bootstrap, and Bayesian methods. Bayesian contours provided in these figures are obtained using `pypolychord`. We have not included results from `emcee` because, as shown in Figure 1, both `emcee` and `pypolychord` lead to largely similar results. From these figures, we find the following. First, across all models, two-dimensional contours obtained with the Bayesian method are broader and hence more conservative. An exception to this is the Jackknife contour for  $h$  and  $M$ , which shows high positive correlation. Moreover, we see that the standard deviations of  $h$  and  $M$  are high, allowing for a smaller value of  $H_0$ . Second, for the case of the flat  $\Lambda$ CDM model, we find that Planck's estimate of  $H_0$  is within  $3 - \sigma$  of the bias-corrected Jackknife estimate. We also note that the Jackknife bias-corrected value of  $\Omega_m$  is more than  $2\sigma$  lower than the GLS or Bayesian estimate. Third, the overlap of confidence contours obtained using Jackknife with those of other methods is fairly high for  $\Lambda$ CDM, flat  $\Lambda$ CDM, and flat  $w$ CDM models, which have only three to four parameters. However, for models  $w$ CDM and flat  $w_0 w_a$ CDM model, which has five

parameters, certain Jackknife confidence contours, in particular those involving  $\Omega_m$ ,  $\Omega_{\text{DE}}$  and  $w_0$ , deviate from corresponding contours obtained using other methods. This is more evident in the flat  $w_0 w_a$ CDM model. In this context, it should be noted that the Jackknife bias for  $\Omega_m$ ,  $\Omega_{\text{DE}}$ ,  $w_0$ , and  $w_a$  is high. Finally, we note that some Bootstrap contours involving these parameters exhibit a multimodal structure. This is clear, for instance, in the  $\Omega_m - w_0$  or  $\Omega_{\text{DE}} - w_0$  confidence contours in the case of  $w$ CDM model and in  $\Omega_m - w_0$  contour of flat  $w_0 - w_a$ CDM model. We can also see multimodality in the Bootstrap probability distributions of  $\Omega_m$ ,  $\Omega_{\text{DE}}$  and  $w_0$  in  $w$ CDM and in  $\Omega_m$  and  $w_a$  of flat  $w_0 w_a$ CDM model.

We have also plotted the corner plot for all models obtained using `pypolychord` in Figure 5. This plot helps us to compare and understand the extend to which different models are constrained. We find that flat  $\Lambda$ CDM is the best constrained by PPS dataset. We also note that Bayesian constraints on  $h$  and  $M$  are independent of the model. It should be noted that this is true for all methods that is considered in this work (see Table II).

## VI. SUMMARY AND DISCUSSION

In this article, we constrained models of dark energy using the PPS dataset and various statistical techniques. We studied flat and non-flat  $\Lambda$ CDM,  $w$ CDM and flat  $w_0 w_a$ CDM models. We used five different statistical methods, which include three frequentist methods, *viz.* GLS, Jackknife, and Bootstrap, and two Bayesian methods, namely MCMC and nested sampling. The MCMC sampling was performed using `emcee` and nested sampling using `pypolychord`. We have provided a brief discussion about various dark energy models in Section II, the PPS dataset in Section III, and statistical techniques in Section IV. We believe these discussions will serve as a quick, easily accessible reference in the literature.

We obtained best-fit values and the standard deviations of different model parameters using GLS. We then employed Jackknife and Bootstrap to estimate bias in the GLS estimate and computed the corrected estimates of model parameters. We also computed Jackknife and Bootstrap estimates of standard deviation. Further, we used both Bayesian methods to calculate the marginalised mean and standard deviation of the parameters. We also computed and plotted correlations between parameters and their probability distributions using different methods. The corner plots (see Figures 1, 2, 3, and 4) that allow us to compare constraints obtained using different methods are a highlight of this work. Finally, in Figure 5, we compare constraints on all models obtained using `pypolychord`. We have highlighted our observations on these calculations and figures in Section V.

We now conclude the manuscript by discussing some of the features mentioned in Section V. First, the Jackknife method estimates a high correlation between  $h$  and  $M$ . This is also reflected in the larger standard deviation of these parameters. It is a known fact that  $h$  and  $M$  are correlated, and the SH0ES dataset was added to break this degeneracy. Perhaps the high positive correlation observed with the Jackknife method indicates that including the SH0ES dataset does not sufficiently break this degeneracy. Second, the Jackknife analysis throws some interesting light on the Hubble tension (see, for instance, [5]). In particular, for the flat  $\Lambda$ CDM model, the Planck estimate of  $H_0$  is within  $3 - \sigma$  of the corresponding Jackknife estimate. It may be argued that the  $N - 1$  factor present in the numerator of Eqn. 4.9, makes the Jackknife estimates rather conservative. But we note that this is unlikely to be the reason. For instance, the error bar on  $\Omega_m$  is actually slightly smaller than that obtained with GLS. Moreover, if we look at confidence contours between pairs  $h$  and  $\Omega_m$ , and between  $M$  and  $\Omega_m$ , Bayesian contours are broader than those of the Jackknife. We believe that the positive correlation between  $h$  and  $M$  may be leading to this broader probability distribution. Third, the bias is high for some of the parameters in models with five parameters,

namely the  $w$ CDM and flat  $w_0 w_a$ CDM models. This indicates that the data is insufficient to properly constrain these models. Further, for these models, Bootstrap shows multimodality in some parameters. Analysing data using different techniques is a good practice. It may help us find out inconsistencies in an analysis. The inconsistencies we found between these methods need further investigation. We believe further studies, probably with better data, are needed to resolve them.

---

[1] S. Perlmutter et al. Measurements of  $\Omega$  and  $\Lambda$  from 42 High Redshift Supernovae. *Astrophys. J.*, 517:565–586, 1999.

[2] Adam G. Riess et al. Observational evidence from supernovae for an accelerating universe and a cosmological constant. *Astron. J.*, 116:1009–1038, 1998.

[3] P. J. E. Peebles and Bharat Ratra. The Cosmological Constant and Dark Energy. *Rev. Mod. Phys.*, 75:559–606, 2003.

[4] M. Abdul Karim et al. DESI DR2 results. II. Measurements of baryon acoustic oscillations and cosmological constraints. *Phys. Rev. D*, 112(8):083515, 2025.

[5] Eleonora Di Valentino, Olga Mena, Supriya Pan, Luca Visinelli, Weiqiang Yang, Alessandro Melchiorri, David F. Mota, Adam G. Riess, and Joseph Silk. In the realm of the Hubble tension—a review of solutions. *Class. Quant. Grav.*, 38(15):153001, 2021.

[6] Jie An, Baorong Chang, and Lixin Xu. Cosmic Constraints to the  $w$ CDM Model from Strong Gravitational Lensing. *Chin. Phys. Lett.*, 33(7):079801, 2016.

[7] Eleonora Di Valentino. Crack in the cosmological paradigm. *Nature Astron.*, 1(9):569–570, 2017.

[8] Rafael J. F. Marcondes and Supriya Pan. Cosmic chronometers constraints on some fast-varying dark energy equations of state. 11 2017.

[9] Michel Chevallier and David Polarski. Accelerating universes with scaling dark matter. *Int. J. Mod. Phys. D*, 10:213–224, 2001.

[10] Eric V. Linder. Exploring the expansion history of the universe. *Phys. Rev. Lett.*, 90:091301, 2003.

[11] Dan Scolnic et al. The Pantheon+ Analysis: The Full Data Set and Light-curve Release. *Astrophys. J.*, 938(2):113, 2022.

[12] Dillon Brout et al. The Pantheon+ Analysis: Cosmological Constraints. *Astrophys. J.*, 938(2):110, 2022.

[13] João Rebouças, Diogo H. F. de Souza, Kunhao Zhong, Vivian Miranda, and Rogerio Rosenfeld. Investigating late-time dark energy and massive neutrinos in light of DESI Y1 BAO. *JCAP*, 02:024, 2025.

[14] Hanyu Cheng, Eleonora Di Valentino, Luis A. Escamilla, Anjan A. Sen, and Luca Visinelli. Pressure parametrization of dark energy: first and second-order constraints with latest cosmological data. *JCAP*, 09:031, 2025.

[15] Drishti Sharma, Purba Mukherjee, Anjan A. Sen, and Suhail Dhawan. Exploring the Impact of Systematic Bias in Type Ia Supernova Cosmology Across Diverse Dark Energy Parametrizations. 11 2025.

[16] Shubham Barua and Shantanu Desai. Constraints on dark energy models using late Universe probes. *Phys. Dark Univ.*, 49:101995, 2025.

[17] Bradley Efron. *The Jackknife, the Bootstrap and Other Resampling Plans*. Philadelphia, Pa. : Society for Industrial and Applied Mathematics, 1982.

[18] Tibshirani Robert J. Efron Bradley. *An Introduction to the Bootstrap*. Macmillan Publishers Limited, 1993.

[19] Jun Shao and Dongsheng Tu. The jackknife and bootstrap. 1996.

[20] W. K. Hastings. Monte Carlo Sampling Methods Using Markov Chains and Their Applications. *Biometrika*, 57:97–109, 1970.

[21] John Skilling. Nested sampling for general Bayesian computation. *Bayesian Analysis*, 1(4):833–859, 2006.

[22] T. Padmanabhan. *Theoretical Astrophysics*. Cambridge University Press, 2002.

[23] Varun Sahni. Dark matter and dark energy. *Lect. Notes Phys.*, 653:141–180, 2004.

[24] T. Padmanabhan. Darker side of the universe ... and the crying need for some bright ideas! In *29th*

*International Cosmic Ray Conference*, 10 2005.

[25] Edmund J. Copeland, M. Sami, and Shinji Tsujikawa. Dynamics of dark energy. *Int. J. Mod. Phys. D*, 15:1753–1936, 2006.

[26] Sean M. Carroll. The Cosmological constant. *Living Rev. Rel.*, 4:1, 2001.

[27] M. G. Dainotti, G. Bargiacchi, M. Bogdan, S. Capozziello, and S. Nagataki. On the statistical assumption on the distance moduli of Supernovae Ia and its impact on the determination of cosmological parameters. *JHEAp*, 41:30–41, 2024.

[28] R. J. Barlow. *Statistics: A Guide to the Use of Statistical Methods in the Physical Sciences (Manchester Physics Series)*. WileyBlackwell, reprint edition, 1989.

[29] T. Padmanabhan and T. Roy Choudhury. A theoretician’s analysis of the supernova data and the limitations in determining the nature of dark energy. *Mon. Not. Roy. Astron. Soc.*, 344:823–834, 2003.

[30] Coralia Cartis, Jan Fiala, Benjamin Marteau, and Lindon Roberts. Improving the Flexibility and Robustness of Model-Based Derivative-Free Optimization Solvers. 3 2018.

[31] M. H. Quenouille. Problems in Plane Sampling. *The Annals of Mathematical Statistics*, 20(3):355 – 375, 1949.

[32] M. H. Quenouille. Notes on bias in estimation. *Biometrika*, 43(3/4):353–360, 1956.

[33] David W. Hogg, Jo Bovy, and Dustin Lang. Data analysis recipes: Fitting a model to data. 8 2010.

[34] Avery McIntosh. The jackknife estimation method, 2016.

[35] B. Efron and C. Stein. The Jackknife Estimate of Variance. *The Annals of Statistics*, 9(3):586 – 596, 1981.

[36] B. Efron. Bootstrap Methods: Another Look at the Jackknife. *The Annals of Statistics*, 7(1):1 – 26, 1979.

[37] D. S. Sivia and J. Skilling. *Data Analysis: A Bayesian Tutorial*. Oxford University Press, Oxford, 2 edition, 2006.

[38] D. Foreman-Mackey, D. W. Hogg, D. Lang, and J. Goodman. emcee: The mcmc hammer. *PASP*, 125:306–312, 2013.

[39] Antony Lewis. GetDist: a Python package for analysing Monte Carlo samples. *JCAP*, 08:025, 2025.

[40] Andrew Gelman and Donald B. Rubin. Inference from Iterative Simulation Using Multiple Sequences. *Statist. Sci.*, 7:457–472, 1992.

[41] W. J. Handley, M. P. Hobson, and A. N. Lasenby. PolyChord: nested sampling for cosmology. *Mon. Not. Roy. Astron. Soc.*, 450(1):L61–L65, 2015.

[42] W. J. Handley, M. P. Hobson, and A. N. Lasenby. POLYCHORD: next-generation nested sampling. *Mon. Not. Roy. Astron. Soc.*, 453(4):4384–4398, November 2015.

[43] N. Aghanim et al. Planck 2018 results. VI. Cosmological parameters. *Astron. Astrophys.*, 641:A6, 2020. [Erratum: *Astron. Astrophys.* 652, C4 (2021)].